International Journal of Mechanics and Energy (IJME)
Vol. 1, Issue 3, 2013, ISSN: 2286-5845

Numerical investigation of three-dimensional thermosolutal convection in a cubic enclosure under magnetic field

Chamseddine Maatki *, Kaouther Ghachem, Lioua Kolsi, Mohamed Naceur Borjini, Habib Ben Aiissia
Unité de Métrologie et de Systèmes Energétiques, National School of Engineers of Monastir (ENIM), University of Monastir (UM), Route Ibn Al Jazzar, Monastir, 5030, TUNISIA,

Abstract: In the present study, thermosolutal convection of fluid in a cubic enclosure filled with a binary mixture is numerically investigated in a strong magnetic field. The physical model is heated from left-hand side vertical wall and cooled from opposing wall. Above this enclosure an electric coil is set to generate a magnetic field. The numerical method in the present work is the formalism vector potential vorticity in a three-dimensional configuration using the finite volume method. The influence of the intensity of magnetic field on the three-dimensional flow, the distributions of temperature and concentration and the characteristics of heat and mass transfer are revealed. The results show that the magnetic force has significant effect on the three-dimensional flow structure and heat and mass transfer.

Keywords: Convection, thermosolutal, hydromagnetic, three-dimensional.

1. Introduction

Double-diffusive convection during phase change in binary mixtures has been the subject of a number of investigations Beghein et al. [1], Costa [2] et Trevisan et Bejan [3]. The definition of double diffusive convection has been confined to cases in which the diffusivities differ considerably and two buoyant forces oppose each other. The considerable differences in diffusivities between heat and salt have exhibited many interesting double diffusive convection phenomena, such as salt fingers and sharp diffusive interfaces. The double diffusive natural convection carried out in a two dimensional cavity filled with a binary fluid and subjected to horizontal temperature and concentration gradients with cooperating volume forces has been researched by Gobin and Bennacer [4]. They have shown that for a high number of Lewis, the thermal transfer goes down as the buoyancy ratio increase.

The analytical and numerical study of double-diffusive natural convection in a horizontal rectangular enclosure subjected to uniform heat and mass flux is carried out by T. Makayssi et al.[5]. Indeed, the authors proposed an analytical solution based on the approximation of parallel flow in the case of a shallow cavity. This analytical solution has good agreement with the numerical solution.

N. Nithyadevi and Yang [6] studied the effect of double-diffusive natural convection of water in a partially heated enclosure with Soret and Dufour coefficients around the density maximum. The effect of the various parameters (thermal Rayleigh number, center of the heating location, density inversion parameter, Buoyancy ratio number, Schmidt number, and Soret and Dufour coefficients) on the flow pattern and heat and mass transfer has been depicted.

The coupling of transient double diffusive convection with radiation is investigated numerically in a square cavity filled with a mixture of N2 and CO2 by A. Ibrahim and D. Lemonnier [7]. Their numerical results show that gas radiation modifies the structure of the velocity and thermal fields and accelerates the convergence to steady state in aiding case, while it

Nomenclature

$\vec{B} = \frac{\vec{B}'}{B_0}$	magnetic field
$C = (C'-C'_l)/(C'_h-C'_l)$	dimensionless species concentration
C'$_h$	High species concentration
C'$_l$	low species concentration
D	species diffusivity
$\vec{e}_X$	Magnetic field Direction
G	Acceleration gravity
Ha	Hartmann number
$\vec{J} = \vec{J}'/(\sigma.\upsilon_0.B_0^2)$	Dimensionless current density
L	cavity side
Le	Lewis number
N	Buoyancy ratio
$\vec{n}$	Unit vector normal
$T = (T'-T'_c)/(T'_h-T'_c)$	dimensionless temperature
$t = t'\alpha / L^2$	dimensionless time
T'$_h$	hot wall temperature
T'$_c$	cold wall temperature
$\vec{u} = \vec{u}'.L/\alpha$	dimensionless velocity
Grecs symbols	
α	thermal diffusivity
β_T	coefficient of thermal expansion
β_C	coefficient of compositional expansion
Φ	dimensionless electric potential
μ	dynamic viscosity
ν	kinematic viscosity
σ_e	electrical conductivity
$\vec{\omega} = \vec{\omega}'\alpha / l^2$	dimensionless vorticity
$\vec{\psi} = \vec{\psi}'/\alpha$	dimensionless stream function
Superscripts	
‘	dimensional variable

favours the generation of instabilities and delays the arrival to a stable solution in opposing one.

An extension of a compressible flow model to double-diffusive convection of binary mixtures of ideal gas enclosed in a cavity is presented by H. Sun et al [8]. Their problem formulation is based on a low Mach number approximation. The authors analyzed the influence of density variation on transient solutions for pure thermal or pure solutal convection as well as for thermosolutal convection in the special case where the thermal and solutal buoyancy forces are equal in intensity either for aiding or for opposing cases.

Yok-Sheung Li et al. [9] studied the transition to chaos in double-diffusive Marangoni convection in a rectangular cavity with horizontal temperature and concentration gradients. They found that the supercritical solution branch takes a quasi-periodicity and phase locking route to chaos while the subcritical branch follows the Ruelle–Takens–Newhouse scenario.

A few of studies are interested in the 3D double diffusive natural convection. Bergeon and Knobloch [10] have studied bifurcations in the double diffusive convection in three dimensional cavity subjected to horizontal temperature and concentration gradients. They’ve proved that in certain conditions, the flow is unstable and the rate is periodic. In fact, the mechanism responsible for these oscillations is identified and the oscillations turned up to be an indirect consequence of the presence of a bifurcation to the longitudinal structures of the three dimensional flow which do not exists in a two dimensional formulation.

Recently, Sezai and Mohamad [11] have demonstrated that, in case of a cube-shaped cavity, the structure of the flow of the thermosolutale natural convection, in the opposite case for values of buoyancy number superior to the unit, is purely three dimensional for certain values of the used parameters such as the buoyancy forces, the thermal Raleigh and the Lewis numbers. They’ve noticed a variety of bifurcations and the formation of complex flow configurations.

More recently, the transient thermosolutal convection in a cubical enclosure having finite thickness walls filled with air, submitted to temperature and concentration gradients, is studied numerically by Geniy V. Kuznetsov et al. [12]. They analyzed the

effect of Rayleigh number and the conductivity ratio on heat and mass transfer.

Similarly, the effect of the magnetic field on thermal convection within rectangular cavity has been studied by many authors. In fact, Oreper and Szekely [13] have demonstrated that the presence of a magnetic field is an important factor determining the quality of the crystal. Ali J. Chamkha and Hameed Al-Naser [14] studied the hydromagnetic double-diffusive convection in a rectangular enclosure with opposing temperature and concentration gradients. They observed an oscillation in the flow in the absence of the magnetic field for a specific range of buoyancy ratio values where the Prandtl number Pr = 1, the Lewis number Le = 2, the thermal Rayleigh number 10^5, and the aspect ratio equal 2 for the enclosure. They find that the heat and mass transfer mechanisms and the flow characteristics inside the enclosure depended strongly on the strength of the magnetic field. In addition the effect of the magnetic field was found to reduce the heat transfer and fluid circulation within the enclosure.

By studying double-diffusive convection during alloyed semiconductor crystal growth in strong axial and transverse magnetic fields, Farrel and Ma [15] mentioned that magnetic field must be strong enough to eliminate flow oscillations but which moderately damped the melt motion in order to achieve both lateral and axial compositional uniformity in the crystal.

Recently, Sarris and al [16] find that, in the presence of a magnetic field, the flow as well as the rate of heat and mass transfer is considerably affected. M. N. Borjini et al [17] studied the effect of radiative heat transfer on the hydromagnetic double-diffusive convection in two-dimensional rectangular enclosure for fixed Prandtl, Rayleigh, and Lewis numbers, $Pr = 13.6$, $Ra = 10^5$, $Le = 2$. Uniform temperatures and concentrations are imposed along the vertical walls while the horizontal walls are assumed to be adiabatic and impermeable to mass transfer. They proved that when progressively varying the optical thickness, multiple solutions are obtained which are steady or oscillatory accordingly to the initial conditions.

Double-diffusive convective flow in a rectangular enclosure with the upper and lower surfaces being insulated and impermeable is studied numerically by Mohamed A. Teamah [18]. In addition, a uniform magnetic field is applied in a horizontal direction. The numerical results are reported for the effect of thermal Rayleigh number, heat generation or absorption coefficient and the Hartmann number on the contours of streamline, temperature, and concentration as well as the dimensionless density.

The originality of this work is to highlight the influence of the buoyancy forces on the three dimensional aspect of the flow as well as on the characteristics of the whole heat and mass transfer in the presence of a magnetic field in a cube-shaped cavity filled with a binary mixture (aqueous solution).

2. Mathematical formulation and numerical method

The geometry under consideration is a cubic cavity (side L), filled with a binary mixture. Different temperatures and concentrations are specified between the left (T'_h, C'_h) and right vertical walls (T'_C, C'_l), and zero heat and mass fluxes are imposed on the remaining walls with no slip boundary conditions for all velocity components fig1. A coil is set above and coaxially with the enclosure to produce magnetic field. The flow is assumed to be laminar and the binary fluid is assumed to be Newtonian and incompressible. The physical properties of the fluid are supposed to be constant and the Boussinesq approximation is adopted. Finally, the Soret and Dufour effects are assumed to be negligible and magnetic Reynolds number is assumed so small that the induced magnetic field is insignificant. The displacement currents, induced

*** Corresponding author:** Chemseddine Maatki
E-mail: maatkichems@yahoo.fr

magnetic field, dissipation and Joule heating are also neglected.

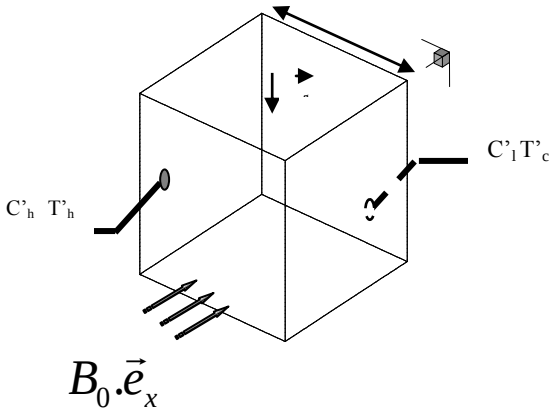

Fig. 1 . The physical model and coordinate system

The dimensionless variables used in this work are:

$$x=\frac{x'}{L},\quad y=\frac{y'}{L},\quad z=\frac{z'}{L},\quad t=\frac{t'}{\alpha L^2},$$

$$(u_1,u_2,u_3)=\frac{(u'_1,u'_2,u'_3)L}{\alpha},\quad C=\frac{C'-C'_l}{C_h-C_l}\quad \text{and}\quad T=\frac{T'-T'_C}{T_h-T_C}$$

For numerical method we resorted to potential vorticity vector formalism in vector form in a three dimensional configuration (Borjini et al [19]). The potential vector and the vorticity are defined respectively by the two relations below:

$$\vec{\omega}=\vec{\nabla}\times\vec{u} \tag{1}$$

$$\vec{u}=\vec{\nabla}\times\vec{\psi} \tag{2}$$

The adimensional equations of conservation describing the transfer phenomena within the cavity are written in the form:

$$\vec{\nabla}^2\vec{\psi}=-\vec{\omega} \tag{3}$$

$$\frac{\partial\vec{\omega}}{\partial t}+(\vec{u}.\vec{\nabla})\vec{\omega}-(\vec{\omega}.\vec{\nabla})\vec{u}=\mathrm{Pr}\,\vec{\nabla}^2\vec{\omega}+Ra.\mathrm{Pr}\left[\frac{\partial T}{\partial z},0,-\frac{\partial T}{\partial x}\right]$$
$$-Ra.\mathrm{Pr}.N\left[\frac{\partial C}{\partial z},0,-\frac{\partial C}{\partial x}\right]+\mathrm{Pr}.Ha^2.(\vec{\nabla}\times(\vec{j}\times\vec{e}_x)) \tag{4}$$

$$\frac{\partial T}{\partial t}+\vec{u}.\vec{\nabla}T=\vec{\nabla}^2T \tag{5}$$

$$\frac{\partial C}{\partial t}+\vec{u}.\vec{\nabla}C=\frac{1}{Le}\vec{\nabla}^2C \tag{6}$$

$$\vec{j}=-\vec{\nabla}\Phi+\vec{u}\times\vec{e}_x \tag{7}$$

$$\vec{\nabla}^2\Phi=\vec{\nabla}.(\vec{u}\times\vec{B})=-\vec{e}_x.\vec{\omega} \tag{8}$$

Equations {3-8} represent respectively the balance laws of mass, linear momentum, thermal energy, concentration, Ohms laws and the balance laws of electric charge.

The dimensionless parameters figuring in these equations are:

$$Ha=B_0L\sqrt{\frac{\sigma_e}{\rho\nu}}\qquad N=\frac{\beta_c(C_h-C_l)}{\beta_T(T_h-T_C)}\qquad Ra=\frac{g\beta_T(T_h-T_C)L^3}{\nu.\alpha}$$
$$\mathrm{Pr}=\frac{\nu}{\alpha}\qquad Le=\frac{\alpha}{D} \tag{9}$$

They represent respectively: Hartmann number, buoyancy ratio, Rayleigh number, Prandtl number and Lewis number. The temperature and concentration boundaries conditions are given by:

$$T(0,y,z)=0\qquad C(0,y,z)=0\qquad \text{and}\quad \frac{\partial T}{\partial n}=0$$
$$T(1,y,z)=1\qquad C(1,y,z)=1$$
$$\frac{\partial C}{\partial n}=0\qquad \text{on other walls.} \tag{10}$$

The boundaries conditions regarding vorticity and potential vector of velocity [19] are:

For $x=0$ and $x=1$,

$$\omega_1 = 0;\ \omega_2 = -\frac{\partial u_3}{\partial x};\ \omega_3 = \frac{\partial u_2}{\partial x} \quad \text{and} \quad \frac{\partial \psi_1}{\partial x} = \psi_2 = \psi_3 = 0 \qquad \text{(11-a)}$$

For $y = 0$ and $y = 1$

$$\omega_1 = \frac{\partial u_3}{\partial y};\ \omega_2 = 0;\ \omega_3 = -\frac{\partial u_1}{\partial y} \quad \text{and} \quad \psi_1 = \frac{\partial \psi_2}{\partial y} = \psi_3 = 0 \qquad \text{(11-b)}$$

For $z = 0$ and $z = 1$

$$\omega_1 = -\frac{\partial u_2}{\partial z};\ \omega_2 = \frac{\partial u_1}{\partial z};\ \omega_3 = 0 \quad \text{and} \quad \psi_1 = \psi_2 = \frac{\partial \psi_3}{\partial z} = 0 \qquad \text{(11-c)}$$

The boundaries conditions related to velocity, electric potential and current density on the inner surface are:

$$u_1 = u_2 = u_3 = 0;\ \frac{\partial \phi}{\partial n} = 0;\ \vec{j}.\vec{n} = 0 \qquad (12)$$

The local Nusselt and Sherwood numbers, have the following expressions:

$$Nu = \frac{\partial T}{\partial x}\bigg|_{x=0,1}; \qquad Sh = \frac{\partial C}{\partial x}\bigg|_{x=0,1} \qquad (13)$$

The Nusselt and Sherwood average numbers on the walls have the following expressions:

$$\overline{Nu} = \int_0^1\int_0^1 Nu.\partial y.\partial z \qquad \overline{Sh} = \int_0^1\int_0^1 Sh.\partial y.\partial z \qquad (14)$$

Equations [1->8] are discretized using the control volume formulation described by Patankar [20] and adopting a power laws scheme on convection diffusion terms. The system is numerically modelled in FORTRAN. More information on the numerical method is in the work of Borjini et al [19].

Results, given in Table.1, show that a grid size of (51x51x51) satisfies the grid independence. The time step is chosen to be 10^{-4}. The convergence criterion is to reduce the maximum mass residual of the grid control volume below 10^{-5}.

Table 1 Grid dependency for (Ra = 10^5, Pr = 10, Le = 10 and N = -0.5)

N*M*Lz	31x31x31	41x41x41	51x51x51	61x61x61
$\overline{Nu}$	3.734 (7.2%)	3.895 (3.2%)	4.023	4.030 (0.17%)
$\overline{Sh}$	7.174 (2.1%)	7.268 (0.8%)	7.328	7.331 (0.04%)

The numerical code is also validated against the results of other studies for magneto-hydrodynamic buoyancy induced convection in enclosures.

Table 2 Comparison between the present results and literature for (Ra = 10^5, Pr = 1, Le = 2 and N = 1)

Ha	Author	$\overline{Nu}$	$\overline{Sh}$
0	Present result (Chamkha et al. [14])	3.358 (3.319)	4.078 (4.030)
5	Present result (Chamkha et al. [14])	3.247 (3.215)	3.948 (3.909)
10	Present result (Chamkha et al. [14])	3.093 (3.048)	3.853 (3.797)
15	Present result (Chamkha et al. [14])	2.905 (2.868)	3.792 (3.744)
20	Present result (Chamkha et al. [14])	2.539 (2.497)	3.714 (3.652)

The validation of the code in hand has been done by means of the Benchmark solution of the work of Chamkha and Al-Naser [14] who have studied the double diffusive convection in a rectangular cavity in the presence of a magnetic field (Ra = 10^5, Pr = 1, Le = 2 and N = 1). Table 2 shows the values of the average Nusselt and Sherwood numbers obtained when the magnetic field is oriented toward x, for different values of Ha. The difference, between the two results is less than 1.5%.

All the values shown in this table are converted according to the dimensionless of Ali J. Chamkha and al. [14].

3 Results and discussion

3.1 Effect of magnetic field on the flow structure, iso-temperature and iso-concentration

When the buoyancy ratio is low N=-0.5 (fig.2), the flow is mainly conducted by thermal volume forces. On analysing figure 2-a representing the projection of flow lines in the main plan Z=0.5, we note that the flow is characterized by an important thermal vortex in the core region of the cavity shifted toward the right active wall (cold surface with light concentration) and turning clockwise. On this figure, the current lines are not closed and form spirals. The spiral-type flow means that the velocity gradient $\frac{\partial u_3}{\partial z}$ is not nil, indicating the existence of a flow towards Z. This result is shown on particles trajectories. By applying a moderate magnetic field (fig 2-b), we notice that the thermal vortex diminishes in size and becomes close to the hot wall. We note also that the spiral type flow is reduced. For the high numbers of Hartmann (fig2-c), flow lines become vertical. In fact, the effect of Lorentz forces increase and the flow structure undergoes great changes.

When the compositional buoyancy forces diminishes to -2 (fig 3), the direction of the main flow is reversed because of the increase of the solutal effect. In fact, fig 3-a demonstrates that the resulting flow structure is made up, on the one hand, of an anti-rotary main cell structure with two inner vortex situated in the central region of the cavity, caused by solutal compositional forces; and on the other hand, of two thermal vortexes, turning clockwise, situated in the upper and lower parts of the cavity. One notices also the appearance of a thermal cell in the bottom corner of the hot side. However, the three dimensional aspect is accentuated and is manifested by the spiral type flow. By applying a moderate magnetic field (figure 3-b) one notice that the structure of the flow is composed of an anti-rotary solutal cells in the central region of the cavity with one thermal vortexes turning in the positive direction in the upper part of the cavity near the hot, highly concentrated side. One also notices the disappearance of the thermal cell in the down part of the enclosure. For high Ha number values (Ha=70), fig 3-c shows that thermal vortexes disappear and that one solutal cell, with one inner vortex structure, becomes situated in central region of the cavity. In this case, the flow becomes conducted mainly by solutal volume forces.

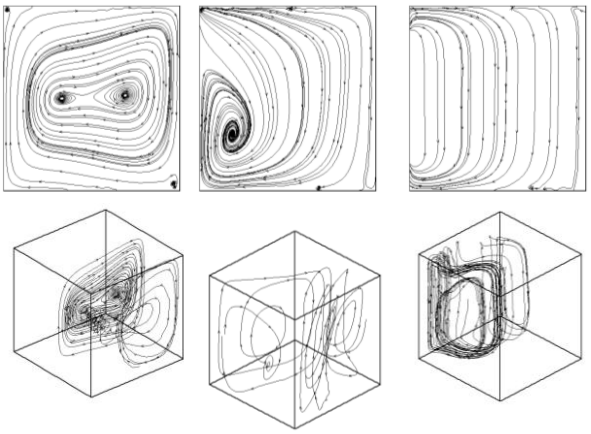

(a) (b) (c)

Fig.2 Projection of flow lines on the mid X-Y plane and some particles trajectories (a: Ha=0, b: Ha=40 and c: Ha=70) for Ra=10^5 and N= -0.5

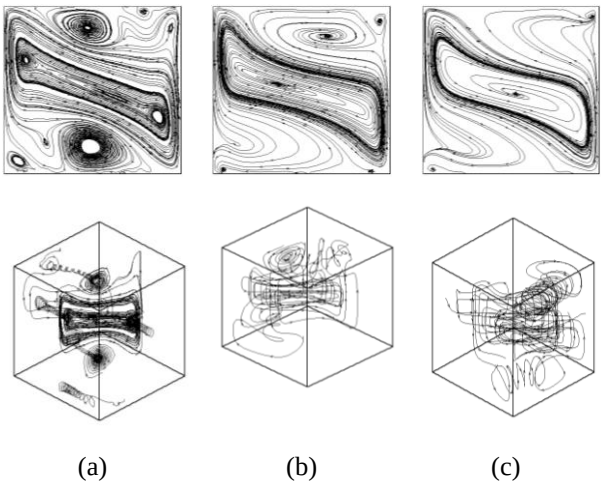

(a) (b) (c)

Fig.3 Projection of flow lines on the mid X-Y plane and some particles trajectories (a: Ha=0, b: Ha=40 and c: Ha=70) for Ra=10^5, and N= -2

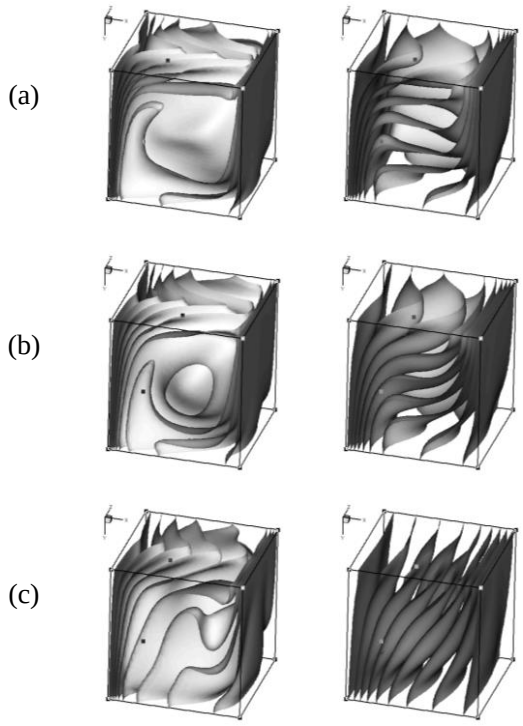

Fig. 4 Iso-surfaces of concentration (on the left) and temperature (on the right) for N=-0.5, (a) : Ha=0 ; (b) : Ha=40 and (c) Ha=80

Figure 4-a (on the left) shows that in the absence of a magnetic field, the iso-concentration are deformed and one observe the zone of inverse gradient of concentration in the core region of the cavity. One notes also that these isosurfaces are vertical and are stacked near the active sides. The solutal gradient is also seen to be high in the lower part of the side with the high concentration and in the upper part of the side with the low concentration. Important distortions of the concentrations isosurfaces are noted due to the three dimensional effects. When the Hartmann number is equals 40, one note that the concentration gradients decrease. One notes also a reduction in the 3D effect. In addition, the variation of the concentration in direction Z diminishes (fig4-b 'left'). In the presence of a strong magnetic field (Ha=70), one note that the iso-concentration become redressed (fig4-c 'left') and the solutal gradient diminishes again near the active walls. However, the variation of the concentration according to direction Z weakens. Consequently, the three dimensional aspect is sensibly reduced.

Figure 4-a 'right', represents the iso-surface of temperature for different Hartmann number. On the one hand, one notes that the isotherms are almost horizontal in the central region of the cavity and thus we have a vertical stratification. On the other hand, one notes that the isotherms are stacked next to the active sides. One notices also that the isotherms are more distorted in the central region of the cavity. By increasing the Hartmann number (figure 4-b 'right'), one note that the vertical stratification weakens and that the temperature gradients near the active sides diminish considerably. Whenever Ha is high (Ha=70, figure 4-c 'right'), the isotherms become vertical with a slight inclination and the thermal gradients diminish more. We observe also that the three dimensional aspect is lessened.

By decreasing the compositional buoyancy ratio to -2, the main flow is reversed. One notice a vertical stratification of concentration inclined and confined in the main flow vortex in the central region of the enclosure (fig 5-a 'left'). The solutal gradient is high near the active sides, in the upper highly concentrated side and in the bottom of the poorly concentrated side. Increase of Hartmann number (Ha=40) shows a decrease in the level of solutal gradient near the active sides (figure 5-b 'left'). One notice also that the variation of concentration in Z direction increases at upper and lower zone while the dimension of the quasi 2D zone is still the same. When Ha =70, one note that the solutal gradient near the active sides weaker fainter and one note as well a reduction of the three dimensional effects. In addition, we observe that the quasi 2D zone in central region is widened and a weak variation of concentration in Z direction at the upper and the lower zone. Fig 5-c'left' shows that this reduction is sharper when the Ha number equal 80.

On fig 5-'right', we have represented the iso-surface of temperature for different Hartmann number. One notes that when the Hartmann number is equal to 0, the

isotherms are vertical with an inclination in the core region of the cavity (fig 5-a 'right'). The intensification of the effect of the magnetic field is characterized, on the one hand, by the decrease of the deformations of the temperature iso-surface in the central region of the enclosure and on the other hand by a small reduction of the temperature gradient near the active sides. By further increasing the number of Ha to 70, one notice that the three dimensional effect is reduced and the central zone with parallel isothermal surfaces become more widened (fig 5-c 'right').

(a)

(b)

(c)

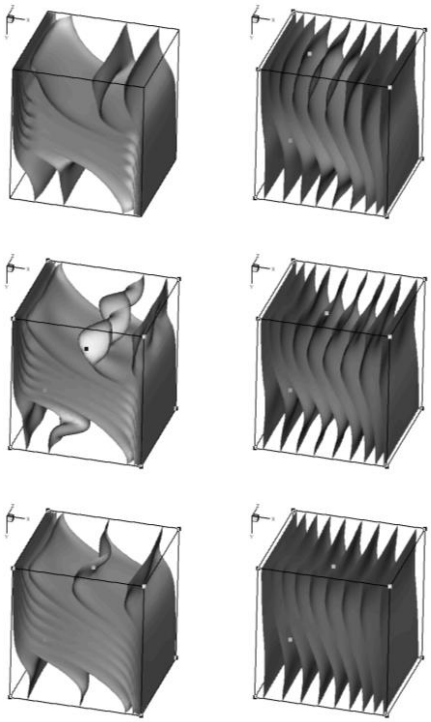

Fig.5 Iso-surfaces of concentration (on the left) and temperature (on the right) for N=-2, (a) : Ha=0 ; (b) : Ha=40 and (c) Ha=80

Where the buoyancy number equal to -0.9, one note that the steady state observed on figure 6 for N = -0.5 and N=-2, disappears in favour of a periodic regimes. Figure 7, shows the development of an oscillatory flow regime when N =- 0.9. In fact Sezai and Mohamad [11] showed, in the case of a cubic enclosure, that the flow regime of double diffusive convection is oscillatory for N ranging between -0.95 and -0.85.

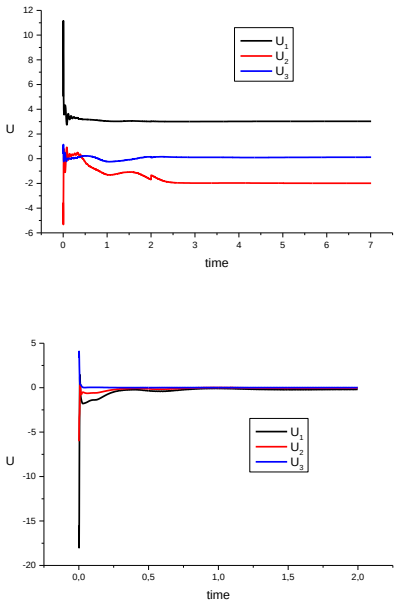

(a)

(b)

Fig. 6 Temporal variations of the component velocity in the center of the cavity for Ha=0, N=-0.5 (a) and N=-2 (b)

By representing the temporal variation of component u_3 in the center of the cavity on figure 7 and the amplitude spectrums on figure 8 and 9, one notice that the moderate increase in the Hartman number (Ha=10), decreases not only the amplitude of the transversal component but also the oscillation frequency.

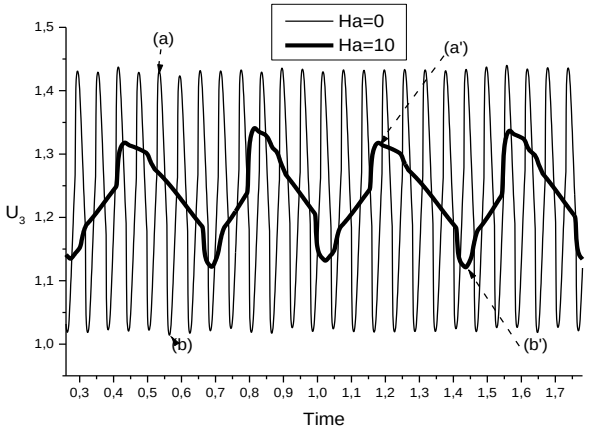

Fig. 7 Temporal variations of the component U_3 in the center of the cavity for different values of Ha (Ha=0 and Ha=10) N=-0.9, and Ra=10^5

The line of the amplitude spectrum in the absence of the magnetic field (fig.8) confirms the existence of a fundamental frequency, of its first harmonic and its

second harmonic respectively equal to f_1=17 , f_2=51 (f_2 =3 f_1) and f3=85 (f_3 =5 f_1).

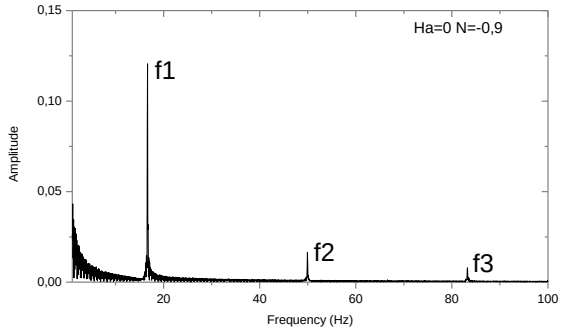

Fig. 8 Spectrum of the velocity component U_3 for N =-0.9, Ra =10^5 and Ha=0

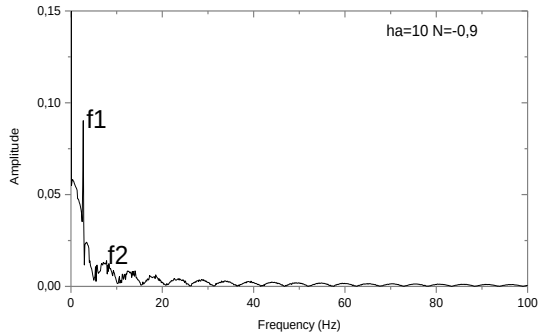

Fig. 9 Spectrum of the velocity component U_3 for N=-0.9, Ra =10^5 and Ha=10

Fig 9 represents the amplitude spectrum of the transversal component of the central velocity when the number of Ha=10. Figure 9 shows the existence of a fundamental frequency f1=2.7 and of its first harmonic f2= 7.4

Figures 10 and 11 represent a projection of flow lines on different planes respectively for Ha=0 and Ha=10. We plotted the main flow in two case simultaneously ((a) , (b)) and((a') , (b')) from figure 7, where ((a) , (a'))with solid lines and ((b) , (b')) with dashed lines. Figures 10 and 11, show that the flow is governed by the thermal volumes forces. The flow structure is characterized by one cell with two vortices in the central region of the cavity. One notes the existence of two solutal cells at the corners near the active walls. Moving from a plane z = 0.5 in plane z = 0.9, we note a coalescence of two vortices. In fact, the flow structure passes from one cell with two vortexes to one cell with one vortex. One notes the persistence of the two solutal cells near the active walls.

Moreover, we observe in figure 10 and 11, that the main flow structure remains unchanged in either case (minimum and maximum) of oscillatory value of transverse component U_3 respectively for Ha=0 and Ha=10 (figure 7). Moreover a slight variation in the flow lines is noticed. Indeed, this result is explained by the low value of the transverse component U_3 against axial and longitudinal components U_1, U_2. Therefore, the flow oscillations are three dimensional original.

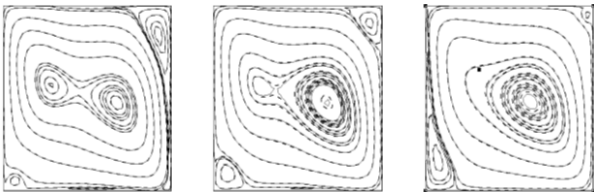

Fig.10 Projection of flow lines on the X-Y plane Z=0.5 (left), Z=0.7 (middle) and Z=0 .9 (right) for Ra=10^5, Ha=0 and N= -0.9. {(a) line, (b) dashed line from figure 7}

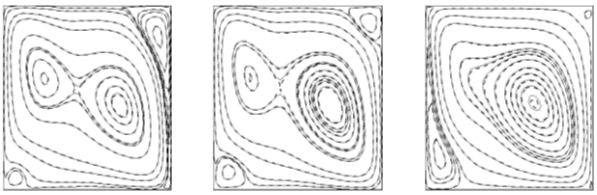

Fig.11 Projection of flow lines on the X-Y plane Z=0.5 (left), Z=0.7 (middle) and Z=0 .9 (right) for Ra=10^5, Ha=10 and N= -0.9. {(a') line, (b') dashed line , from figure 7}

Figure 12, represents the temporal evolution of the component^{u_3} in the centre of the cavity. It shows that for high Hartmann numbers (Ha=40 and Ha=70), the flow rate becomes chaotic.

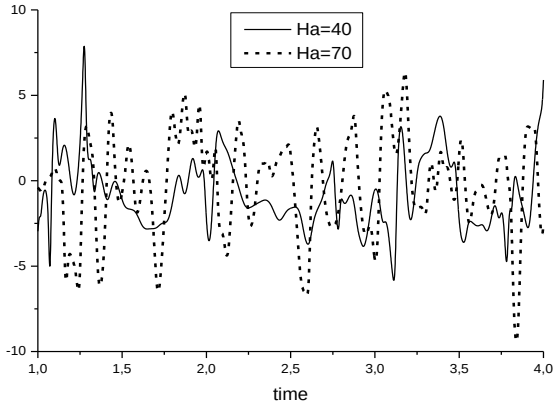

Fig.12 Temporal evolution of component U_3 in the center of the enclosure for various values of Ha (Ha= 40 and 70), N=-0.9 and Ra=10^5

3.2 Effect of magnetic field on the heat and mass transfer:

Analysis of figure 13 draws the attention to the fact that with the increase of the intensity of the magnetic field, the heat and mass transfer decrease. Therefore, in the absence of a magnetic field the average number of Nusselt is Nu= 4.27, which undergoes a decrease of 73% when the number of Hartmann reaches 80. The average Sherwood number decreases by 65% moving from a Hartmann number equal to 0 until Ha =80. These results are a good agreement with Chamkha et al. [14] who reported that the presence of a magnetic field reduces heat and mass transfer.

Fig 14 shows that in this particular case where the volume forces are dominant (N=-2), the intensification of the magnetic field brings about only a small decrease in heat and mass transfers. In fact, even with high Ha values, the number of average Nusselt take on values close to 1.4 and the number of average Sherwood take on values close to 5 reaching a decline of 30% compared to the case where there is no magnetic field.

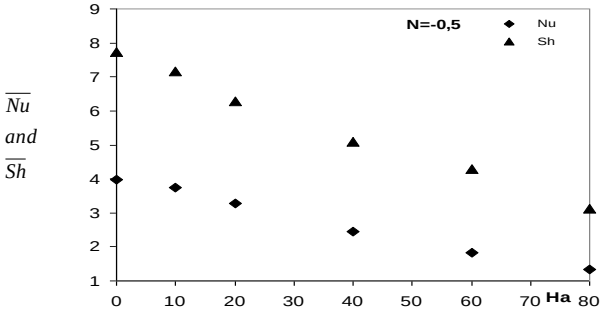

Fig. 13 Variation of average Sherwood and Nusselt numbers according to Ha for N=-0.5

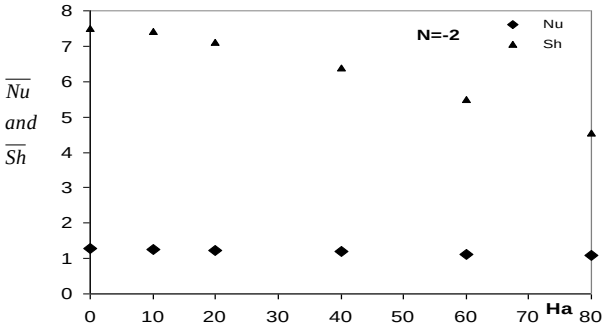

Fig. 14 The average Nusselt and Sherwood numbers according to Hartmann number, N=-2

4. Conclusion

In the present work we attempt to model the three dimensional aspects of thermosolutal natural convection in a cubic enclosure subject to horizontal and opposing gradients of heat and solute in presence of magnetic field. Different behaviors of flow were observed when changing Ha for different N. The main findings of the present investigation can be summarized as follows:

- For N=-0.5

A monotonic reduction of intensities of main and three dimensional transverse flows is observed when Ha increase.

Elimination of thermal stratification in the core region of the cavity.

A reduction of temperature and concentration gradients near active walls. This implies a reduction of heat and mass transfer.

- For N=-2

When Ha is greater than 40, a reduction of 3D flow structure is observed. So that it is suggested to avoid a moderate Hartmann value when utilizing magnetic field for damping the 3D flow.

In this case, we notes there is no great effect of Ha on heat and mass transfer.

- An oscillatory flow is observed for N=-0.9.

We demonstrated that the flow oscillations are 3D aspect.

One notice that the moderate increase in the Hartman number (Ha=10), decreases not only the amplitude of the transversal component but also the oscillation frequency.

For a strong magnetic field, the flow rate becomes chaotic.

References

[1] Beghein, C., Haghighat, F., & Allard, F. (1992). Numerical study of double-diffusive natural convection in a square cavity. International Journal of Heat and Mass Transfer, 35(4), 833–846.

[2] Costa, V. A. F. (1997). Double-diffusive natural convection in a square enclosure with heat and mass diffusive walls. International Journal of Heat and Mass Transfer, 40(17), 4061–4071.

[3] Trevisan, V. O., & Bejan, A. (1992). Combined heat and mass transfer by natural convection in a vertical enclosure. International Journal of Heat and Mass Transfer, 109, 104–112.

[4] D. Gobin and R. Bennacer; Cooperating thermosolutal convection in enclosures II. Heat transfer and flow structure Int. J. Heat Mass Transfer. Vol. 39, No. 13, pp. 2683-2697, 1996

[5] T. Makayssi, M. Lamsaadi, M. Naïmi, M. Hasnaoui, A. Raji, A. Bahlaou ; Natural double-diffusive convection in a shallow horizontal rectangular cavity uniformly heated and salted from the side and filled with non-Newtonian power-law fluids: Energy Conversion and Management, Volume 49, Issue 8, August 2008, Pages 2016-2025

[6] N. Nithyadevi, Ruey-Jen Yang ; Double diffusive natural convection in a partially heated enclosure with Soret and Dufour effects , International Journal of Heat and Fluid Flow, Volume 30, Issue 5, October 2009, Pages 902-910

[7] A. Ibrahim, D. Lemonnier ; Numerical study of coupled double-diffusive natural convection and radiation in a square cavity filled with A N2–CO2 mixture International Communications in Heat and Mass Transfer, Volume 36, Issue 3, March 2009, Pages 197-202

[8] H. Sun, G. Lauriat, D.L. Sun, W.Q. Tao; Transient double-diffusive convection in an enclosure with large density variations ;International Journal of Heat and Mass Transfer, Volume 53, Issue 4, 31 January 2010, Pages 615-625

[9] Yok-Sheung Li, Zhi-Wu Chen, Jie-Min Zhan ; Double-diffusive Marangoni convection in a rectangular cavity: Transition to chaos ; International Journal of Heat and Mass Transfer, Volume 53, Issues 23-24, November 2010, Pages 5223-5231

[10] Bergeon et E. Knobloch, Natural doubly diffusive convection in three-dimensional enclosures, Physics of fluids ,Volume 14 Number 9 , 2002

[11] Sezai, A.A. Mohamad, Double diffusive convection in a cubic enclosure with opposing temperature and concentration gradients, Phys. Fluids 12 (2000) 2210-2223.

[12] Geniy V. Kuznetsov, Mikhail A. Sheremet; A numerical simulation of double-diffusive conjugate natural convection in an enclosure ; International Journal of Thermal Sciences, Available online 1 June 2011

[13] G.M. Oreper, J. Szekely, The effect of an externally imposed magnetic field on buoyancy driven flow in a rectangular cavity, J. Cryst. Growth 64 (1983) 505–515.

[14] A.J. Chamkha, H. Al-Naser, Hydromagnetic double-diffuse convection in a rectangular enclosure with opposing temperature and concentration gradients, Int. J. Heat Mass Transfer 45 (2002) 2465– 2483.

[15] M.V. Farrell, N. Ma, Macrosegregation during alloyed semiconductor crystal growth in strong axial and transverse magnetic fields, Int. J. Heat Mass Transfer 47 (2004) 3047–3055.

[16] Sarris, I. E., Kakarantzas, S. C., Grecos, A. P., & Vlachos, N. S. (2005). MHD natural convection in a laterally and volumetrically heated square cavity. International Journal of Heat and Mass Transfer, 48, 3443–3453.

[17] M. N. Borjini, Habib Ben Aissia, Kamel Halouani, Belkacem Zeghmati, Effect of optical properties on oscillatory hydromagnetic double-diffusive convection within semitransparent fluid, International Journal of Heat and Mass Transfer, 49, 21-22, 3984-3996

[18] Mohamed A. Teamah. Numerical simulation of double diffusive natural convection in rectangular enclosure in the presences of magnetic field and heat source International

Journal of Thermal Sciences, Volume 47, Issue 3, March 2008, Pages 237-248

[19] M. N. Borjini, K. Lioua, N. Daouas, and H. Ben Aı¨ssia, Hydromagnetic Double-Diffusive Laminar Natural Convection in a Radiatively Participating Fluid, Numer. Heat Transfer A,vol. 48, pp. 483–506, 2005.

[20] S.V Patankar, Numerical Heat transfer and Fluid Flow, Hemisphere Publishing Corporation, Taylor and Francis Group, New York, 1980, pp. 113e137.